

Neutron Imaging

Tobias Neuwirth*¹ and Michael Schulz^{†1}

¹Technical University of Munich, Heinz Maier-Leibnitz Zentrum (MLZ),
Lichtenbergstr. 1, 85748 Garching, Germany

14. January 2020



*Tobias.Neuwirth@frm2.tum.de

†Michael.Schulz@frm2.tum.de

Contents

1	Introduction to Neutron Imaging	3
1.1	Applications of neutron imaging	3
1.2	Aim of the experiment	3
2	Interaction between matter and neutrons	3
2.1	Neutrons	3
2.2	Absorption, refraction and scattering	4
2.2.1	Absorption and Refraction	4
2.2.2	Scattering	5
3	Neutron Imaging	6
3.1	Neutron Imaging -Basics-	6
3.2	Spatially resolved detection of neutrons	7
3.3	Tomography	8
4	Experimental details	10
4.1	ANTARES	10
4.2	Instrument control	12
5	Experimental tasks	13
5.1	Focusing the detector/Analyzing the resolution	14
5.2	Spatial resolution	14
5.3	Beer–Lambert law	15
5.3.1	White beam measurements	15
5.3.2	Monochromatic measurements	16
5.4	Neutron tomography	16
6	Data Evaluation	16
7	Experimental report	17
7.1	General structure	17
7.2	Analysis tasks	17
7.2.1	Analysis of the spatial resolution	17
7.2.2	Analysis of the step wedges	18
7.2.3	Tomography reconstruction and analysis	19
A	Table of neutron cross-sections	20

1 Introduction to Neutron Imaging

1.1 Applications of neutron imaging

Neutron imaging (NI) is a method allowing to perform a nondestructive analysis of the inner structure of an object [1]. Unlike X-ray cross-sections, neutron cross-sections do not show a quadratic dependence on the atomic number. This is a result of their interaction with the atomic core instead of the electronic shell. For instance some light elements like hydrogen or lithium show low transmission in neutron imaging, because of a large scattering cross-section or absorption cross-section, respectively. In contrast, some heavier elements like aluminum and lead show higher transmission. Even isotopes of the same element can have radically different total neutron cross-sections. An example for this is helium. The rare isotope ^3He has a high total neutron cross-section and is used as a detector material for neutrons. In contrast, ^4He has a very low total neutron cross-section and is used to reduce the neutron loss during transit from the reactor to the experiments. Due to its complementary contrast mechanism, neutron imaging is often used in materials science, cultural heritage research, archaeology and engineering, when X-ray imaging fails to produce sufficient contrast.

1.2 Aim of the experiment

The aim of this experiment is to give you a practical introduction to neutron imaging. It will be shown how various parameters influence the resolution of a neutron imaging beamline. The influence of polychromaticity on measurement results, as well as the limits of the Beer-Lambert-law will be experimentally evaluated. A neutron tomography will be performed, showing the possible uses of this technique.

2 Interaction between matter and neutrons

2.1 Neutrons

Neutrons are electrically neutral baryons composed of two down and one up quarks. Together with protons, they constitute the nuclei of atoms. As a result of these properties, neutrons interact with the nucleus, but not the electron hull. Furthermore, due to their interaction only with the (small) atomic core, they typically have a high penetration depth into materials. As neutrons are particle waves, they can be either described as a wave or a particle, which leads to an equivalence of velocity v_n , wavelength λ_n (de Broglie wavelength) and energy E_n :

$$E_n = \frac{1}{2}m_n v_n^2 \quad (1)$$

and

$$\lambda_n = \frac{h}{m_n v_n} . \quad (2)$$

Here $m_n = 1.675 \times 10^{-27}$ kg is the neutron mass, while $h = 6.626 \times 10^{-34}$ Js is the Planck constant.

Moreover, neutrons have a magnetic moment. Accordingly, neutrons may also be used to probe magnetic properties of samples.

2.2 Absorption, refraction and scattering

Neutrons interacting with matter can either be absorbed, refracted or scattered. As neutron imaging analyzes the transmission of neutrons through a sample, absorption and scattering are the two interactions which need to be further considered. In contrast, refraction of neutrons at material borders can be ignored for the scope of this experiment, as the index of refraction for nearly all materials is very close to unity.

As noted above, neutron imaging analyzes the transmission, which is governed by the Beer-Lambert-Law:

$$T = \frac{I_f}{I_i} = \exp \left[\int -(\Sigma_{\text{abs}}(z) + \Sigma_{\text{sca}}(z)) dz \right]. \quad (3)$$

Here Σ_{abs} and Σ_{sca} are the linear absorption coefficient and the linear scattering coefficient, respectively¹ and z is the position in beam direction. Assuming the sample is composed of a single element or a homogeneous alloy, the line integral can be simplified to the following:

$$T = \frac{I_f}{I_i} = \exp [-(\Sigma_{\text{abs}} + \Sigma_{\text{sca}}) t], \quad (4)$$

where t is the sample thickness in beam direction. The linear scattering coefficient can be further broken down into a coherent (Σ_{coh}) and an incoherent (Σ_{inc}) component. Σ can be calculated from the microscopic cross-section σ using the following equation

$$\Sigma = \frac{\sigma}{V_m} N_A = \frac{\rho}{M} N_A \sigma. \quad (5)$$

Here V_m is the molar volume of the considered element, $N_A = 6.022 \times 10^{23} \text{ mol}^{-1}$ the Avogadro constant, ρ the density of the considered element and M the molar mass of the considered element. It is important to note that in most cases the microscopic cross-section is given in units of Barn ($\text{b} = 10^{-28} \text{ m}^2$), while the linear absorption/scattering coefficient is given in cm^{-1} . In [2] the cross-sections of most elements including their isotopes are tabulated. In Tab. 1 the most important cross-sections for the following experiment have been tabulated. In the following, we will look a bit more in depth at the absorption and scattering cross-sections.

2.2.1 Absorption and Refraction

As noted before the transmission of neutrons through a sample depends on the absorption cross-section of the material. The exact absorption cross-section for every element and even every isotope is governed by the structuring of the atomic core. Hence, unlike X-rays, the absorption cross-section of neutrons does not rise with increasing atomic mass. In many cases, this allows to use neutrons and x-rays as complementary imaging techniques, one offering contrast where the other does not work. For the following experiments, the

¹In neutron physics the linear coefficients are often called the macroscopic cross-section.

absorption cross-section will be the most important quantity to consider. It is very important to note that the absorption cross-section depends on the wavelength and are typically tabulated for a wavelength of 1.8 \AA (see Table 1). In the wavelength range we consider in our experiments (1.3 \AA to 6.0 \AA), the cross-section has a $1/v$ dependence. Effectively, this allows us to calculate the cross-section for every wavelength $\Sigma_{\text{abs}}^\lambda$ using the following equation:

$$\Sigma_{\text{abs}}^\lambda = \Sigma_{\text{abs}} \frac{\lambda}{1.8 \text{ \AA}} \quad (6)$$

Please be aware, this $1/v$ dependence is not correct for short wavelengths ($\lambda \ll 1 \text{ \AA}$) as well as some heavy elements.

2.2.2 Scattering

A further aspect of neutron interaction with matter is the scattering of neutrons. In the case of imaging, the scattering aspect is in most cases secondary to absorption. Neutrons can be described as a wave using the Schroedinger equation, which allows to describe the wave function of an undisturbed ψ_i and a scattered neutron ψ_f , respectively, in the following way:

$$\psi_i = \psi_0 e^{ikz} \quad (7)$$

$$\psi_f = \psi_0 f(\lambda, \theta) \frac{e^{ikr}}{r} = \psi_0 (-b) \frac{e^{ikr}}{r} \quad (8)$$

The incoming neutron is described as a planar wave in z-direction, while the scattered neutron is considered a spherical wave. ψ_0 is the amplitude of the wave, r the radius of the outgoing spherical wave and k denotes the wave number, which is constant during elastic scattering. $f(\lambda, \theta)$ denotes the probability of a neutron of a certain wavelength λ being scattered under an angle θ . For neutrons this is denoted as the scattering length ($-b$) and depends on the nuclear and magnetic form factor and the spin of the neutrons. Scattering may either be coherent or incoherent. Coherent scattering depends on the correlation between the positions of the same nucleus at different times and on the correlation between the position of different nuclei at different times. Hence, the scattered waves ψ_f generated by every nuclei result in an interference pattern. In contrast, incoherent scattering depends only on the correlation between the position of the same nucleus at different times. As a result no interference pattern is generated [3]. For both coherent and incoherent scattering the neutron may either scatter elastically, exchanging no energy with the scattering centers, or inelastically, gaining or losing energy. Elastic coherent scattering allows to access information about the structure of the crystal lattice. Inelastic coherent scattering gives information about collective excitations in a sample, such as phonons and spin waves. Further reading on the scattering process can be found in [3]

3 Neutron Imaging

3.1 Neutron Imaging -Basics-

Neutron imaging is a completely different method of analyzing materials compared to neutron scattering, hence the instrumentation is very much different from standard scattering experiments. In its basic configuration an imaging instrument, in our case ANTARES, is a pinhole camera. In Fig. 1 the basic setup is sketched. The neutron source, normally the moderator around the fuel element, is on the same axis as the pinhole, the sample and the spatially resolved neutron detector.

Typically, neutron imaging instruments do not employ refractive lenses to focus the neu-

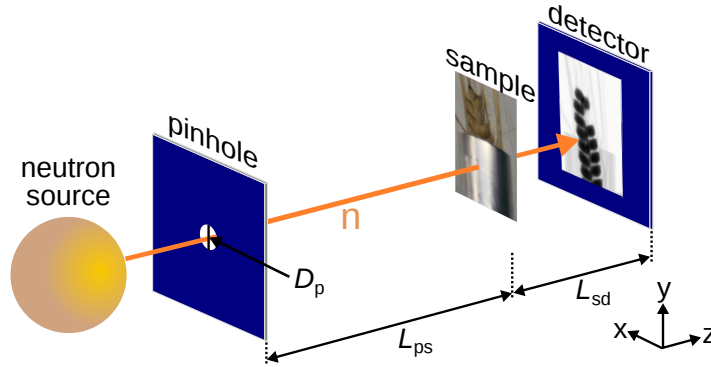


Figure 1: Pinhole camera principle of an imaging beamline. Pinhole, sample and detector are all on the same axis. Adapted from [4]

tron beam. This is a result of the very small difference of the index of refraction from unity for most materials. As a result, lenses tend to be very thick (meters) in beam direction resulting in a high attenuation of neutrons. Hence, only a pinhole camera geometry is usable. This results in a lower limit of achievable spatial resolution which is governed by the geometry of the instrument. The achievable spatial resolution of the instrument depends on the pinhole diameter D_p , the distance between pinhole and sample L_{ps} and the sample-to-detector-distance (SDD) L_{sd} as shown in Fig. 2. Effectively, with these parameters the maximum smearing diameter d_D of one point of the sample on the detector can be described as

$$d_D = \frac{D_p}{L_{ps}} L_{sd}. \quad (9)$$

Often, the value which is used to describe the achievable spatial resolution is the collimation ratio, which is defined as $L/D = \frac{L_{pd}}{D_p}$, where L_{pd} is the distance between pinhole and detector. Looking at Eq. 9 it is clearly visible that increasing L_{ps} , decreasing L_{sd} or decreasing D_p leads to less smearing on the detector. As a rule of thumb L_{sd} should be kept as small as possible. In contrast, choosing L_{ps} and D_p is not as simple as changing them, does not only result in a change of resolution but also changes the available neutron flux. As there are no optics in an imaging beamline, an increase in resolution always leads to an decrease in flux and vice versa. Hence, a compromise between available flux and achievable resolution has to be found. The aforementioned spatial resolution is often called the

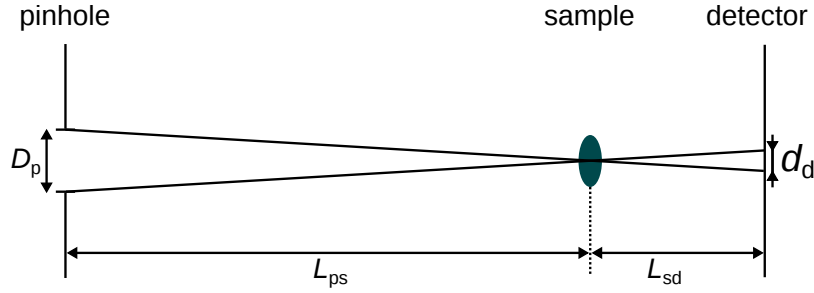


Figure 2: Graphical depiction of Eq. 9. A point in the sample is smeared out on the detector depending on the pinhole-to-sample distance L_{ps} , the sample-to-detector-distance (SDD) L_{sd} and the pinhole diameter D_p . Adapted from [4]

geometrical resolution and is only a part of the true instrument resolution. The instrument resolution is a convolution of the geometric resolution, the optical resolution of the detector and the smearing of the scintillator. The latter contributions will be explained in more detail in the following section.

The information acquired by neutron imaging is the transmission of neutrons (T) through a sample. The detector systems typically used for neutron imaging do not provide absolute neutron count values, but values proportional to the neutron count. Furthermore, the neutron beam and also the detection system is not homogeneous over the area illuminated by the neutron beam. This means even without a sample the values detected by the system vary over the field of view of the detector. Hence, in addition to the data image containing the the sample a second image without the sample has to be taken. This open beam image (ob) contains the same inhomogeneities as the data image, just without the sample. Additionally, the camera of the detector system has a certain thermal noise and offset. These two components are an additive component in both the data and the ob image. Hence, an image containing this offset called the dark image (di) has to be acquired. Using the data, ob and di the transmission of neutrons can be calculated. This process is called normalization:

$$T = \frac{\text{data} - \text{di}}{\text{ob} - \text{di}} \quad (10)$$

A more in depth explanation of the detector system will follow in the next section.

3.2 Spatially resolved detection of neutrons

State-of-the-art spatially resolved neutron imaging detection systems typically use a detector comprised of three parts: a scintillation screen, an optical lens and a CCD/CMOS camera. The scintillation screen is a material which transforms neutrons into light in the visible spectrum. The material used in most cases is LiF:ZnS doped with Cu. We will not go into full detail how the specific nuclear processes in a scintillation screen work. In short, the LiF absorbs the neutrons, emitting an α -particle which travels through the scintillation material and excites electrons in the ZnS. The excited electrons will then fall back to their ground state by emitting light. One of the most important characteristic of a scintillation screen is its thickness, as this defines the fraction of the neutrons absorbed, the achievable

resolution and the light-output of the scintillation screen. A thicker scintillation screen absorbs more neutron and hence has a higher light output, but loses in spatial resolution. In Fig. 3 these relations are illustrated.

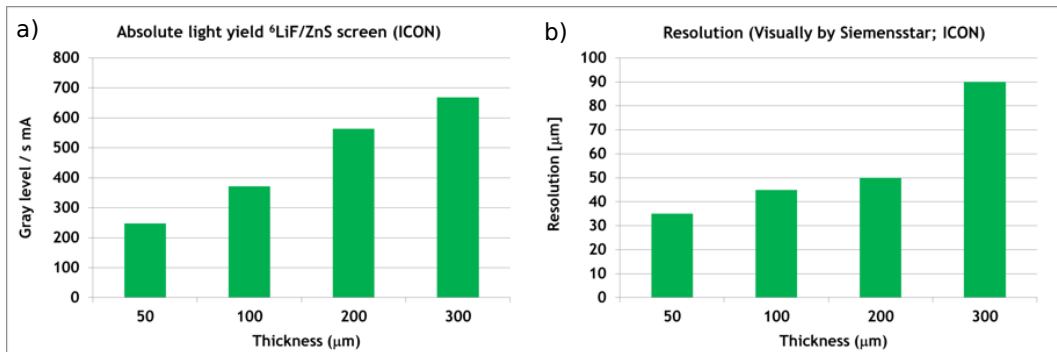


Figure 3: a) Dependence of the light output of the scintillator on the thickness. A higher thickness leads to a higher light output b) Dependence of the scintillator resolution on the thickness of the scintillator. A smaller thickness leads to a better spatial resolution. Taken from [5].

The optic of a detector system consists of one or two mirrors and a lens. The mirrors are used to remove the camera from the direct neutron beam, reducing the noise and protecting the camera from radiation damage. The magnification of the lens and the pixel size of the camera determine the effective pixel size of the detector system. The minimum resolvable structure size is double the effective pixel size. For the resolutions considered in this experiment, we can assume that the lens does not contribute significantly. For high resolution imaging this assumption is not valid.

The camera is either a cooled CCD-camera (charge-coupled device) or a cooled CMOS-camera (complementary metal-oxide-semiconductors). The cooling reduces the thermal noise present in the camera. This is especially important in neutron imaging, as during long exposure times (approx. 60 s) the thermal noise quickly adds up. While the cameras are shielded against radiation, there is still an increased noise in the acquired images. This noise is mostly caused by gamma radiation. If gamma radiation directly hits the camera sensor, a bright spot will appear in the acquired image at this position. Such spots are generally much brighter than the surrounding area. These spots are called gamma spots and have to be eliminated from the image during the data processing. To do this there are various image filtering techniques which can be used.

While it is possible to calculate the achievable resolution using the relations shown above, in practice the resolution is often determined experimentally. The determination of the resolution is part of the experimental tasks you will perform.

3.3 Tomography

As computed tomography (CT) is not the primary aim of the experiment, only a short overview over the theory is given. For a more in depth view of CT please refer to the advanced lab course No. 79 covering X-ray computed tomography or take a look at the book

Principles of computerized tomographic imaging by Kak and Slaney [6].

Using neutron tomography, one can resolve the total linear neutron attenuation coefficient Σ_{att} inside a sample in 3D. As noted in the theory section, when taking an image (projection), one essentially gets the intensity value $I(x,y)$ after the sample defined by the line integral along the neutron path.

$$I(x,y) = I_0(x,y) \exp - \int \Sigma_{\text{att}}(x,y,z) dz \quad (11)$$

To get the information about the attenuation at a position (x,y,z) in the sample, the sample is rotated and projections under different angles are recorded. Doing this gives the line integral for a projection under different angles θ . A sketch of this process is presented in Fig. 4. The projections are related by the Radon transform to the spatial distribution of

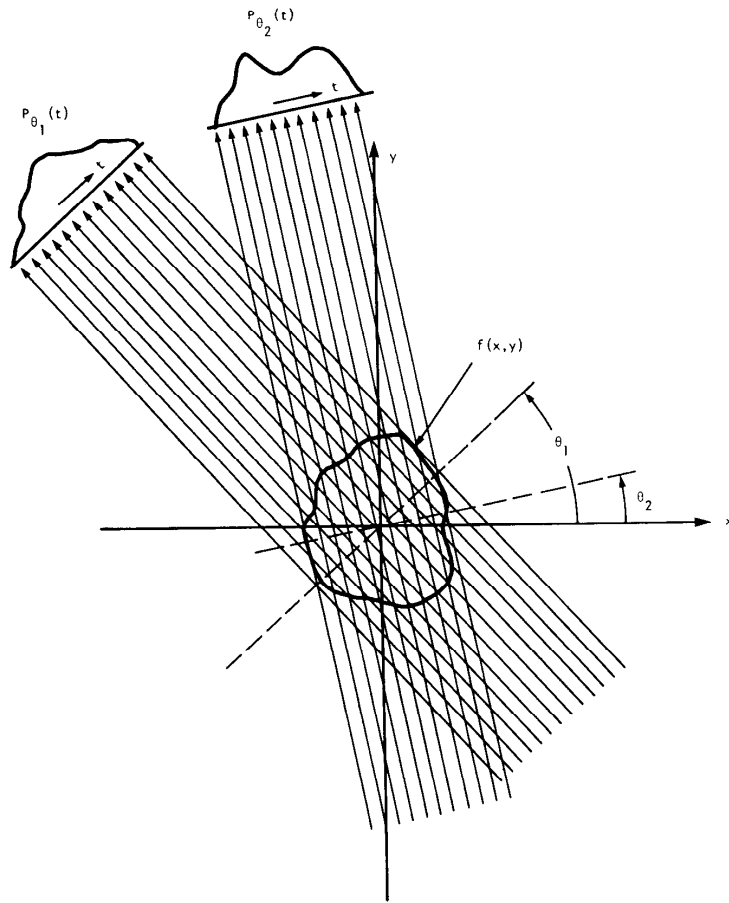


Figure 4: Parallel projections are taken for a number of different angles. Taken from [6].

the attenuation coefficient $\Sigma(x,y,z)$ inside the sample. The set of measured projections for different angles θ is called the sinogram. By inverting the Radon transform, the $\Sigma(x,y,z)$ distribution inside the sample can be recovered. This is called the inverse Radon transform. However, this simple inversion causes blurring in the reconstructed 3D data. Hence, typically an algorithm called the filtered backprojection (FBP), which is a fast and robust

analytic reconstruction algorithm, is used. For FBP one first performs a fourier transformation for every projection, then multiplies the transformed projection with a filter kernel. Afterwards, the filtered projections is transformed back into the spatial domain. As a last step the filtered projection is projected in the image plane.

4 Experimental details

4.1 ANTARES

The instrument with which you will be performing the experiments described in Sec. 5 is the imaging instrument ANTARES located at the SR 4a beamport of the FRM II reactor at Heinz Maier-Leibnitz Zentrum. In the following this instrument and the important components for the experiments will be shortly described. In Fig. 7 the positions of the explained devices in the instrument are shown.

The first component we will talk about is the shutter system, which allows to open and close the neutron beam. ANTARES has three shutters. Shutter 1 is located in the wall of the reactor pool and is used to shut off the neutron beam when the instrument isn't used for a longer period of time. Shutter 2 is the instrument shutter and is used to shut off the beam, when performing short changes of the instrument setup i.e. sample changes. The third shutter is the Fast shutter. This shutter is used to shut off the neutron beam between image acquisitions, helping to reduce the amount of activation and radiation damage on the components of ANTARES. **Please note: If you want to enter measurement chamber 1 or 2, Shutter 2 needs to be closed. Closing Shutter 1 is not enough to enter the measurement chambers. If you need to enter the beam preparation area, Shutter 1 and Shutter 2 need to be closed.**

As noted above the achievable resolution of the instrument depends on the collimation of the neutron beam, which can be changed by changing the pinhole diameter or the distance between pinhole and detector. As the distance between detector and pinhole is fixed in most cases the pinhole diameter of ANTARES can be varied. In neutron imaging, the pinhole is typically extended in beam direction and is then called a collimator. The extension in beam direction allows to better define the divergence of the neutrons allowed to pass through. This helps to reduce background, as neutrons which do not conform to the expected neutron flight path are stopped before the instrument. The collimation of ANTARES can be easily varied by exchanging the collimator with another. This can be done automatically. The possible D_p 's are 35.68 mm, 17.80 mm, 8.92 mm, 4.45 mm and 2.00 mm. You will use a pinhole diameter D_p of 35.68 mm and 17.8 mm .

The incoming neutron beam into ANTARES is called a white beam as it has the full neutron energy spectrum as defined by the cold neutron source. In Fig. 5 the spectrum is shown.

As noted before, the absorption and scattering cross-sections are wavelength dependent. Hence to be able to analyze this dependence, the energy of the incoming neutron beam has to be known. As a result ANTARES has two possible devices to select certain wavelengths for the experiments, the neutron velocity selector (NVS) and the double-crystal-monochromator. For the planned experiments only the NVS will be used, hence this device will be focused on. The NVS is effectively a fast rotating turbine whose turbine

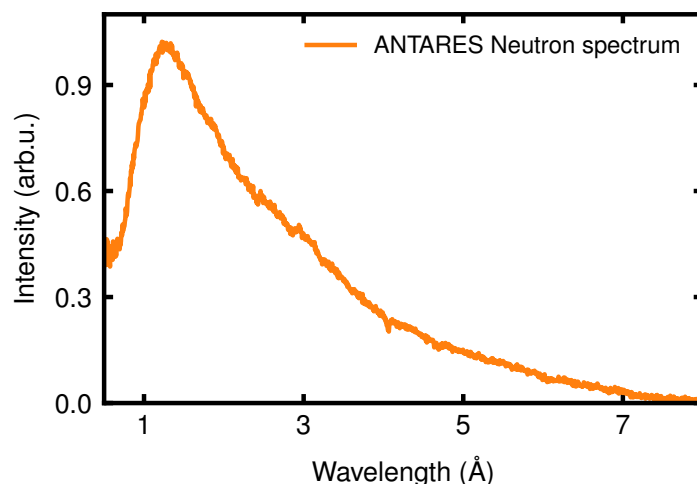


Figure 5: Incoming neutron wavelength spectrum of ANTARES.

blades are made of neutron absorbing materials. In Fig. 6 such a turbine is shown. due to the wave-particle duality of neutrons, a neutron wavelength can be assigned a neutron velocity. As an example a neutron with a wavelength of 1.8 \AA has a velocity of 2200 m s^{-1} . As one can imagine, depending on the rotational velocity of the NVS neutrons having a certain velocity can pass through the NVS without being absorbed². The wavelength resolution $\frac{\Delta\lambda}{\lambda}$ is roughly 10 %.

Velocity Selector



Figure 6: Turbine of a neutron velocity selector.

While neutrons travel through air, they are scattering off the hydrogen contained in the humidity in the air causing a loss of roughly 1 % to 3 % of neutrons per meter. To minimize this effect the flight tubes filled with helium are placed in the neutron path. As indicated in Table **cross**, Helium shows a very small absorption cross section for neutrons, making it an ideal medium to reduce the attenuation of the neutron beam on its flight path through the instrument.

The beam of ANTARES reaches a maximum size of 30 cm by 30 cm. In case of smaller

²A nice video of this process can be found here: <https://www.youtube.com/watch?v=jjPg59qxH3k>

samples, such a beam size is unnecessary and only increases the background during measurements. The increase in background is caused by diffuse neutrons in the measurement chamber caused by neutrons scattering off the hydrogen in the air. Hence, ANTARES has the possibility to reduce the neutron beam size using a beam limiter. The beam limiter consists of neutron absorbing lamellae which can be introduced in the neutron beam, to reduce its size and the noise during measurements.

For precise positioning of the samples, we will use the cryomanipulator of ANTARES in combination with an additional linear stage.

The detector we will use, is the High-Resolution detector of ANTARES. This detector can be used in different configurations. For our experiments we will use the medium resolution option which results in a maximum field of view (FoV) of $76\text{mm} \times 76\text{mm}$. In this operation mode the detector uses a LiF-scintillation screen with a thickness of either $50\ \mu\text{m}$ or $100\ \mu\text{m}$. The camera is an ANDOR Neo 5.5 sCMOS camera with a sensor size of $16.6\text{mm} \times 14\text{mm}$ and a pixel size of $6.5\ \mu\text{m}$, which corresponds to 2560×2160 pixels. The effective pixel size on the scintillation screen can be adjusted during focusing of the camera and is typically around $30\ \mu\text{m}$. The lens used is a ZEISS Milvus 2/100 ZF.2.

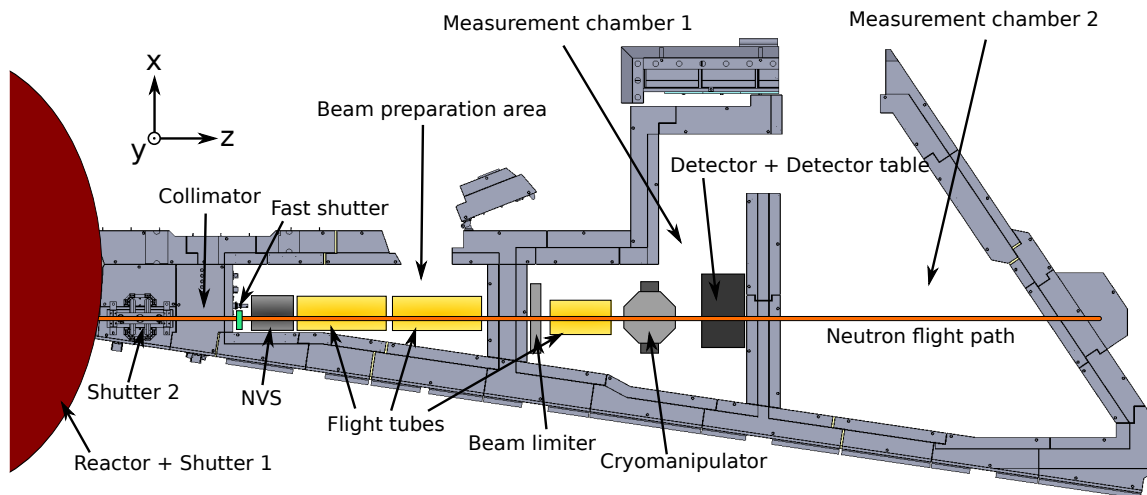


Figure 7: Top view of ANTARES with sketched instrument components.

4.2 Instrument control

Most devices in ANTARES are remote controlled using the **Networked Integrated COntrol System (NICOS)**. In the following, we will shortly give an introduction to NICOS. A detailed explanation will be given directly by your supervisor during the experiment. In Fig. 7 the coordinate system used in ANTARES is shown. The naming convention for devices in ANTARES will be explained on the example of the cryomanipulator. Typically three letter names are used for devices. The first part of an axis name i.e. **c** denotes the component moved i.e. the cryomanipulator. The second part of the denotes if the movement is a

translation **t** or a rotation **r** and the last part gives the axis along which the movement is performed (translation) **x** or around which axis the rotation occurs. Hence, **ctx** is a linear axis of the cryomanipulator, performing a translation along the x-axis. To move a device you can call the device in the comandline of NICOS and give it a value i.e. **move(ctx, 200)**. This command would move the axis **ctx** to the value 200 mm. Please note that normally the value for a linear axis is given in mm, while for a roation axis the value is given in degrees. A further important aspect is that the values given are absolute values. As an example, **ctx** is at 146 mm and you want to move it 60 mm in positive direction, then the command you need to give is **ctx(206)**.

To take an image we use the **count(xx)** command. In the brackets the exposure time (in seconds) can be set. For taking the openbeam images we use the **openbeamimage(t=xx)** command, which is a modified count command, saving the images in a separate folder. Similarly, the **darkimage(t=xx)** command, used for taking darkimages, also saves the images in a separate folder. For taking darkimages it is important to shut off the neutron beam by closing the instrument shutter.

If you need to take images at different positions of an axis, there exist two scan functions which automate this process:

cscan(ctx, 150, 5, 10, t=2)

This command positions the axis **ctx** centred around the value 150 mm with ten steps in both directions with 5 mm between each step and acquire an image at each position with an exposure time of 2 s. This will result in 21 images at positions of **ctx** ranging from 100 mm to 200 mm.

scan(ctx, 150, 5, 10, t=2)

This will scan the axis **ctx** starting from 150 mm taking 10 images each separated by 5 mm. For focusing of the detector there exists a modification of cscan-command shown below.

cscan(scintillatortx, 67, 1, 10, det_sharp, t=2)

This command again positions the axis **ctx** centred around the value 67 mm with ten steps in both directions with 1 mm between each step with an exposure time of 2 s. This will result in 21 images at positions of **ctx** ranging from 57 mm to 77 mm. The addition of the parameter **det_sharp** causes NICOS to calculate the sharpness of every image taken. With the scan-button in the GUI these sharpness values can be plotted and fitted.

move(shutter2, 'closed') and **move(shutter2, 'open')**

These two commands will close and open shutter 2, respectively.

NICOS is based on the programming language python. Hence python scripts can be used to perform complicated measurement procedures. This feature will make a lot of the tasks in this lab course easier. A detailed explanation of the usage of the scripting module will be given by your supervisor.

5 Experimental tasks

In the following, the experimental tasks to be completed during the lab course are described. It is very important to follow the safety instruction provided by your supervisor. Your supervisor will also help you in mounting, dismounting and positioning of the samples. Hence, no detailed description of theses processes will be given. For most experiments

you will also be given prepared measurement scripts where you only have to fill in the positioning data. Again this will be explained in detail by your supervisor. An important detail for all the following measurements is that in addition to the data image (data), an open beam image (ob) and a dark image (di) are needed. While we don't need to take these two images for every data image we take, whenever we change the counting time of the detector or the setup for an image we have to take them. In Sec. 3.1 the reason for acquiring these two images was explained.

5.1 Focusing the detector/Analyzing the resolution

Our first task for the following experiments is to focus the detector. First we need to decide on the necessary FoV. For the intended experiments a FoV of $70\text{ mm} \times 70\text{ mm}$ is necessary. The detector we will use is the detector described in Sec. 4.1 which we adjust to get the necessary FoV. To get this FoV we need to set the lens to the correct focal distance. In our case, we need to move the 1:4 marker on the lens to the upper marker on the camera box. Please note that the colon should be directly on the marker. Then move the focusing axis (**scintillatortx**) to 144 mm. Afterwards make sure that the scintillator is in the center of the neutron beam, the center is marked on the detector table as well as the walls. If it is not in the center adjust the detector table (**dtx**, **dy**) until the scintillator is in the center. For the focusing process we will use a test target made out of Gadolinium, . The target is fixed directly on the scintillator using aluminium tape. Afterwards, you can take images using the **count** command. Try different exposure times and choose one where the detector does not reach saturation. This image will probably be very blurry. Afterwards you can use the modified **cscan** command in NICOS to automatically calculate the sharpness of the acquired images. The usage of the command is described in Sec. 4.2. After you have fitted the resulting curve, you can move the detector to the focused position.

After the focusing we need to check how good the achieved spatial resolution is. For this we can either directly evaluate the test target, which may however be very subjective. Or we calculate the modulation transfer function (MTF), which is more objective. For a first idea about the resolution we will use the Siemens star, but later we will calculate the MTF. Your supervisor will tell you how to evaluate the image of the test target.

5.2 Spatial resolution

One way to calculate the MTF is to place a knife edge test target in front of the detector. A knife edge is a highly absorbing sample with a sharply defined edge. We will use a thin piece of Cadmium as our test target. First we remove the test target as we won't need it for further experiments. To be able to analyze the influence of the SDD on the resolution we will mount the knife edge on the linear stage (**sample_tz**) mounted on the cryomanipulator, allowing us to change the SDD. As noted before, the achievable spatial resolution depends on the collimation of the neutron beam as well as the SDD. In this experiment we will change both of these parameters, to see their effects on the resolution. We will use the two collimators with a pinhole $D_{p,1} = 35.68\text{ mm}$ and with a pinhole $D_{p,2} = 17.8\text{ mm}$, respectively. For each collimator we will perform a scan of the sample-to-detector-distance

(SDD) using the **sample.tz** stage. The travel range for this stage is 300 mm. Please perform a scan with at least ten steps over the full range of the linear stage. For this you can use the **scan** command of NICOS. Ensure that the knife edge target does not collide with anything during the travel. Choose an appropriate exposure time for each image. You will need a higher exposure time for the smaller pinhole. After performing an SDD-scan use the cryomanipulator to move the knife edge out of the detector FoV and take an openbeam image with the same exposure time as a data image. Use the **openbeamimage** command for this. After performing both SDD-scans shut off the neutron beam by closing the instrument shutter and use the **darkimage** command to take a darkimage. Again use the same exposure time you used for the data images.

5.3 Beer–Lambert law

In the following experiment we will verify the Beer-Lambert law. For this you have a number of step wedges made out of different materials. A step wedge is a test sample which has been machined to have a number of different but well defined sample thicknesses. This allows to simultaneously evaluate different sample thicknesses for the same material. In Fig. 8 the geometry of the used step wedges is shown on the example of a brass step wedge. We have a set of step wedges made of different single elements (carbon, magnesium, aluminium, titanium, vanadium, chromium, iron, nickel, copper, zinc, zirconium, niobium, molybdenum, tin, tungsten and lead) as well as composite materials (brass, bronze, invar, PE, PTFE, wood, glass, ferrite and steel) from which you can choose.

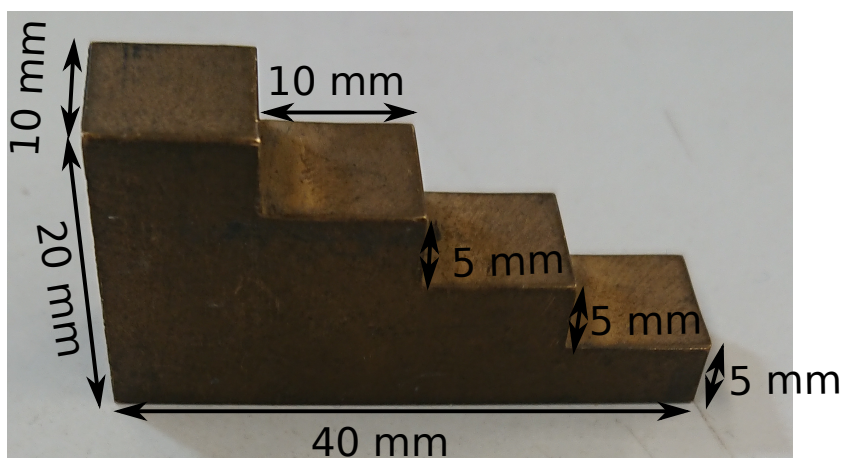


Figure 8: Example of a step wedge

5.3.1 White beam measurements

For the first experiment we will use at least ten of the step wedges described previously. First we need to replace the knife edge target with the step wedges. Afterwards we need to position the step wedges in front of the detector. Make sure that you can move the step wedges fully out of the FoV without crashing into anything. After positioning, take an

image using the **count** command, then move the step wedges out of the beam and take an open beam image. Don't forget to also take a dark image.

5.3.2 Monochromatic measurements

For the next part we will need to use a monochromatic neutron beam. Hence we will use the neutron velocity selector to choose a wavelength. **Start-up of the velocity selector is only done by your supervisor. Doing this wrong has the high danger of destroying the velocity selector.** After the start-up of the velocity selector we can choose a wavelength at which we want to perform the measurements. For the experiment we will use the following wavelengths 3.4 Å, 3.6 Å, 3.8 Å, 4.0 Å, 4.2 Å, 4.4 Å and 4.6 Å. To select a certain wavelength, the velocity selector has to rotate at a certain speed. Therefore, when changing the wavelength we need to wait until the selector has reached the correct speed and stabilizes. For each wavelength we will need to take a data images, as well as an open beam image. Please note that the exposure time for the monochromatic measurements has to be significantly increased as the neutron flux is significantly lower.

5.4 Neutron tomography

As a last part we will perform neutron tomography on an aluminium tube filled with various materials. For this we need to switch from the cryomanipulator to the huber sample stage, as we need a rotation stage for the tomography. For this we will demount the step wedges and move the cryomanipulator out of the beam. Furthermore, we will shut down the NVS and remove it from the beam. Afterwards, we can use the three jaw chuck to fix the aluminium tube in place. First we need to position the aluminium rod in front of the detector. Then we need to consider the number of angles needed to get an acceptable resolution. The rule of thumb is $\frac{\pi}{2} \times$ width of the sample in pixels. Accordingly, we will choose the number of projections. For the tomography itself a script exists, where only the parameters need to be changed.

6 Data Evaluation

After the experimental part of our lab course and before we come to the specific evaluation of the data we need to do some preliminary evaluation. The first step is to remove the gamma spots from all images. As explained above, gamma-spots are the result of gamma-radiation directly hitting the chip of the camera. Such gamma-spots are one of the most important artifacts to eliminate in neutron imaging, hence the first step for evaluation is to filter these gamma-spots. For this purpose we have a gamma-filter tool performing this operation. The gamma filter compares an image with a blurred variant of this image. If the difference in one pixel is larger than a defined threshold, this pixel is seen as a gamma-spot. Depending on the extent of the difference the gamma spot is then filtered by median filters with varying sizes (3×3 , 5×5 or 7×7). After the removal of the gamma-spots we have to take care of the inhomogeneities present in our images, caused by inhomogeneities in the neutron beam, the scintillator and the optics. Correcting these inhomogeneities allows

to recover the true transmission (T), for which we need the data images, open beam (ob) images and the dark images (di) taken during the experiments. After this step the specific evaluation needed for the different experiments can be performed. This will be described further in the following sections.

- Gamma Filter
- Normalization (important Beam inhomogeneity)
- Camera Noise

7 Experimental report

7.1 General structure

We expect you to write approximately 10 pages of experimental report in which you report your results and the conclusions you have reached from the results. Additionally, please write a short chapter on the theories that are needed to understand your results. When discussing your results you should first start with what you did, then describe your results and afterwards discuss them. Also figures should always be linked to your text. This means describe what one can see in the figures to allow the reader to understand your further reasoning without having to go to the figure. Then tell about your conclusions drawn from the figure. Additionally the figure caption needs to explain the figure and should allow the reader to understand the figure without having to look into the text. When preparing graphs always make sure you have both axes labeled clearly as well as enable the reader to easily differentiate between different data sets. This means use highly different colors for the graphs as well as thick enough lines and font sizes. In the following the expected analysis of the data is detailed.

7.2 Analysis tasks

7.2.1 Analysis of the spatial resolution

Here you use the images of the line pattern to determine the resolution. To do this we will use the modulation transfer function (MTF). The MTF is defined as follows:

$$\text{MTF}(f) = \frac{\text{image contrast}(f)}{\text{object contrast}(f)}, \quad (12)$$

where f is the spatial frequency of the modulation. The image contrast is the contrast achieved by the detector system, while the object contrast is the real contrast caused by the test sample. These two values are not readily available, hence a different approach is used. The MTF is also the discrete Fourier transform (DFT) of the line spread function (LSF), which is the response of the imaging system to a sharp line in the image. To get the LSF we will use the the edge spread function (ESF), which is the response of the imaging system

to a sharp edge i.e. the fast transition from a high transmission to a low transmission. The ESF(x,y) in a pixel (x,y) of an image is defined as follows:

$$ESF(x,y) = \frac{I(x,y) - \mu}{\sigma} \quad (13)$$

Here $I(m,n)$ is the intensity of the image at pixel (x,y), μ is the arithmetic average intensity of the image, while σ is the standard deviation of the image. The LSF is then the derivative of ESF perpendicular to the direction of the edge. For an edge in y-direction it follows:

$$LSF(x,y) = \frac{d}{dx}ESF(x,y) \quad (14)$$

Now we can calculate the MTF in x-direction:

$$MTF = \frac{|DFT[LSF(x,y)]|}{\max(|DFT[LSF(x,y)]|)} \quad (15)$$

The MTF is then plotted vs the spatial frequency f , which can be calculated by:

$$f = \frac{1}{N \times p} . \quad (16)$$

Here N is the number of pixels and p is the pixel size in x-direction, respectively. Typically, the spatial resolution is defined as the spatial frequency at an MTF value of 10%. The spatial frequency is typically given in line pairs per millimeter. A line pair means a light and dark line. To get the resolvable structure size of the imaging beamline in micrometers one can use the following formula.

$$\text{Resolution } (\mu\text{m}) = \frac{1000 \frac{\mu\text{m}}{\text{mm}}}{2 \times \text{line pairs per millimeter}} \quad (17)$$

In You will get an incomplete python script for the evaluation of the spatial resolution. After you have calculated the resolution for all images taken during Sec. 5.1 you should then plot the spatial resolution versus the SDD for both collimations. Additionally plot the spatial resolution you expect when you only consider the geometric resolution of the beamline given in Eq. 9. Compare the results. Does it match your expectations? Where do the differences between the geometric resolution and the measured resolution stem from?

7.2.2 Analysis of the step wedges

You should do the following tasks of plotting and fitting always for all step wedges, unless noted otherwise.

White beam without scattering

Here you will analyze the images taken in Sec. 5.3. First lets look at the images taken using the white beam of ANTARES. Plot the transmission value versus the sample thickness t .

Fit the function of the Beer-Lambert law to the transmission T using the assumption there is no scattering only absorption i.e. the fit function looks like this:

$$T = \exp[-(\Sigma_{\text{abs}})t] \quad (18)$$

Does this result in values close to the ones given in Table 1 for the single element samples? Why not? Which step wedges show the best/worst match? Explain.

White beam with scattering

Now try to plot both the raw data points as well as the full Beer-Lambert law using the tabled values for both absorption and scattering. How do the results compare now? Why does it still not fit?

Monochromatic beam

Now let's try the Beer-Lambert law again using a single wavelength (4.6 Å). Again plot both the data points and the theory curve from the Beer-Lambert law using the correction factor for the neutron velocity presented in the Eq. 6. How do the theory and data fit together now?

Now plot the data of one sample thickness versus the wavelength. Also plot the theory curve of the Beer-Lambert law using the correction factor. Why does the theory and the experimental data not fit together in many cases? Take a close look at the Beer-Lambert law. (Hint: There is still something missing in the presented law, which is important in crystalline materials.) Discuss.

Analyzing the material composition

In this part your task is to analyze the material composition of some of the alloyed step wedges using the assumption, that they are not scattering. Step wedges composed of only two materials (brass, bronze, Invar) are for obvious reasons the easiest to analyze, hence we will focus on those. What is the fitting equation we need to use to get the material composition? Which data set should be ideally used for this analysis? Do your values for the composition correspond to the chemical composition given?

7.2.3 Tomography reconstruction and analysis

For the reconstruction of the tomography data we will use either the commercial program Octopus or a free python package depending on the availability of our computing clusters. For the subsequent analysis of the 3D-volume we will use the program VG-Studio Max. For both the reconstruction and the 3D analysis you will be aided by your supervisor. They will explain how to use the programs and what you need to watch out for. As you don't know which materials have been placed inside the aluminium rod, your task is to identify the various materials. In the discussion of your results you should talk about what the tomography allowed you to see inside the sample as well as artifacts you encountered during reconstruction.

References

- [1] Anderson, I. S., McGreevy, R. L., and Hassina, Z. B. *Neutron Imaging and Applications: A Reference for the Imaging Community 2009*. Tech. rep. ISBN 978-0-387-78692-6.
- [2] Sears, V. F. “Neutron scattering lengths and cross sections”. In: *Neutron news* 3.3 (1992), pp. 26–37.
- [3] Squires, G. L. *Introduction to the theory of thermal neutron scattering*. Courier Corporation, 1996.
- [4] Reimann, T. “Vortex matter beyond SANS”. Dissertation. München: Technische Universität München, 2017.
- [5] *RC Tritec*. <https://www.rctritec.com/de/szintillatoren/produkte.html>. Accessed: 14-January-2020.
- [6] Kak, A. C. and Slaney, M. “Principles of computerized tomographic imaging”. In: *The Institute of Electrical and Electronics Engineers, Inc* (1988).

A Table of neutron cross-sections

Element	σ_{abs} (b)	σ_{sca} (b)	σ_{coh} (b)	σ_{inc} (b)
H	0.3326	82.02	1.7568	80.26
He	0.00747	1.34	1.34	0
C	0.00350	5.551	5.550	0.001
N	1.90	11.51	11.01	0.050
O	0.00019	4.232	0.000	4.232
F	0.0096	4.018	4.017	0.0008
Na	0.530	3.28	1.66	1.62
Mg	0.063	3.71	3.631	0.08
Al	0.231	1.503	1.495	0.0082
Si	0.171	2.167	2.1633	0.004
Ti	6.09	4.35	1.485	2.87
V	5.08	5.10	0.01838	5.08
Cr	3.05	3.49	1.660	1.83
Fe	2.56	11.62	11.22	0.40
Ni	4.49	18.5	13.3	5.2
Cu	3.78	8.03	7.485	0.55
Zn	1.11	4.131	4.054	0.077
Zr	0.185	6.46	6.44	0.02
Nb	1.15	6.255	6.253	0.0024
Mo	2.48	5.71	5.67	0.04
Sn	0.626	4.892	4.870	0.022
W	18.3	4.60	2.97	1.63
Pb	0.171	11.118	11.115	0.003

Table 1: Absorption and scattering cross-sections at 1.8 Å for various materials. Taken from [2].